

Novel Electrodeposition Behavior of Ni on Porous Anodic Alumina Templates without a Conductive Interlayer

M. T. Wu, I. C. Leu,* J. H. Yen, and M. H. Hon

Department of Materials Science and Engineering, National Cheng Kung University, 701 Tainan, Taiwan

Received: November 5, 2004; In Final Form: February 6, 2005

During template-assisted electrodeposition, single-crystalline metallic nanowires could be obtained only when the overpotential is low. However, an unusual electrodeposition behavior on the PAA/Si substrate without a conductive interlayer between the template and Si is described in the present study. Through the electrical breakdown of the template, Ni nanodots, nanowires and nanotubes could be obtained by only changing the electrodeposition voltage on the same substrate. The mechanisms leading to the formation of various nanostructures are described in detail and compared with those for the conventional template-assisted electrodeposition process. The electrodeposition first occurred on the pore wall instead of from the underlying substrate, leading to the formation of some Ni nanotubes at a more negative voltage. Besides, single-crystalline Ni nanowires could also be formed even when the electrodeposition voltage was as negative as -40 V, indicating that the formation of single-crystalline metallic nanowires under a large overpotential is possible.

Introduction

Recently, template-mediated growth has become one of the popular methods to fabricate nanostructures over a large area.^{1–3} Well-aligned and dimension-controlled nanostructures can be obtained through the deposition of materials into the nanochannels of a membrane. Among the membrane materials, porous anodic alumina (PAA) is usually used for the template-mediated growth due to its ease of production. By varying the anodization conditions, the characteristics of PAA can be easily controlled.^{4,5} Because of its thermal stability and chemical inertness, the fabrication of nanostructures using PAA as a template can be conducted under many different conditions.

For the template-mediated growth, many processes are adopted to fabricate nanostructures, such as the vapor-, solution-, and electrochemistry-based methods, etc.^{6–8} For the vapor-based methods, the deposition rate is usually too high so that the pore mouths will be closed before the materials can be fully deposited into the channels. For the solution-based methods, the low filling efficiency is the main problem because the capillarity is the only driving force to guide the transport of materials in the channels. For the electrochemistry-based methods (especially for the electrodeposition), the growth of the nanostructures is field-assisted and usually selectively occurs at the conductive area of the substrate, which makes it possible to avoid the closure of the pore mouth and to increase the filling efficiency. Besides, the cost of the sources and the equipments for electrodeposition is relatively low, reducing the capital investment of the whole process. Therefore, the electrodeposition is now considered as a powerful tool for template-mediated growth of nanostructures.

For template-mediated electrodeposition, conventionally, a conductive layer must be coated on one side of the membrane as the electrode for electrodeposition. Without a conductive layer, the filling efficiency of materials into the channels is quite low. Moreover, for the fabrication of one-dimensional nano-

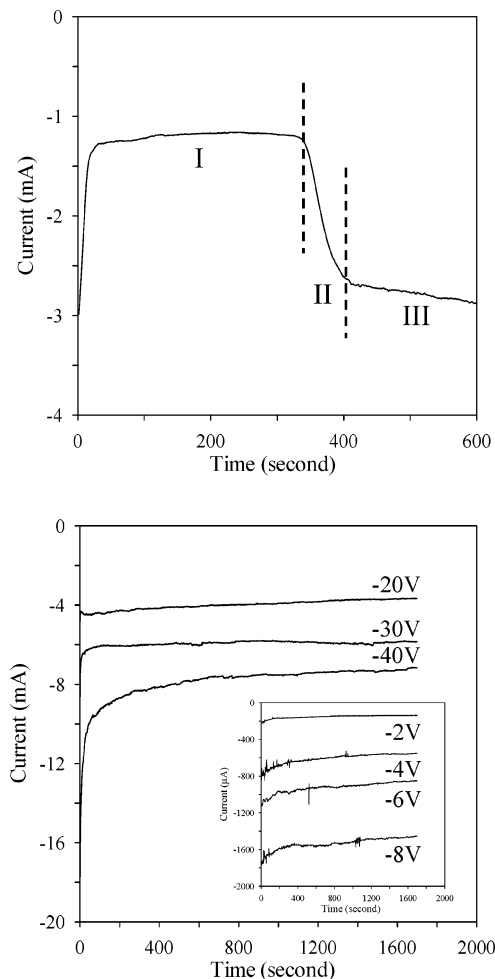


Figure 1. Dependence of the current on electrodeposition time at different voltages on 300 nm thick PAA/Si substrates.

structures, single-crystalline nanowires of Cu, Ag, Au and some low melting point metals (such as Pb and Bi) can be obtained

* To whom correspondence should be addressed. E-mail: icleu@mail.mse.ncku.edu.tw.

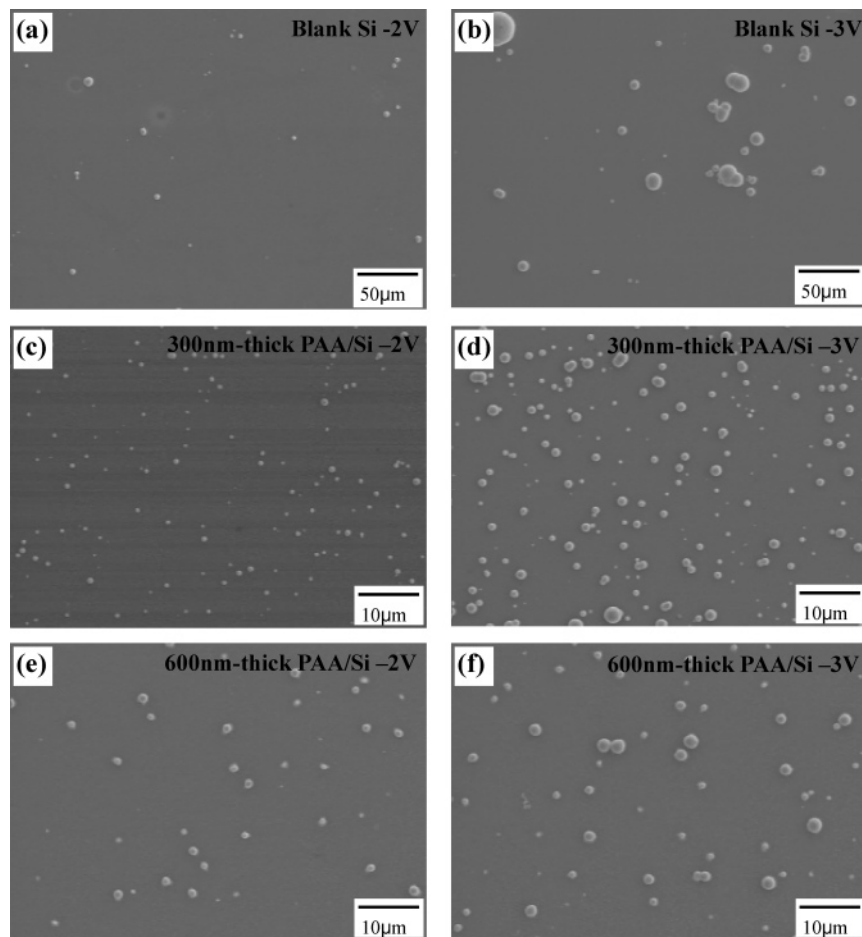


Figure 2. Surface morphologies of the as-electrodeposited substrates [(a) and (b) for the blank Si substrates, (c) and (d) for the 300 nm thick PAA/Si substrates, (e) and (f) for the 600 nm thick PAA/Si substrates). The applied voltage was -2 V for that in images (a), (c) and (e), and was -3 V for that in images (b), (d) and (f).

if a lower overpotential is used during electrodeposition. However, for the high melting point metals such as Ni, Co and Pt, the growth of single-crystalline nanowires via electrodeposition is very difficult and has not been reported till now.^{9,10} In this study, an unusual electrodeposition behavior of Ni is presented, using the PAA on Si without a conductive layer as a template. Ni nanostructures with different aspect ratio could be obtained through this process. The filling efficiency still exceeded 90% even though a conductive layer was not introduced between the PAA and the substrate. Besides, some single-crystalline Ni nanowires were obtained when the electrodeposition was conducted under a large overpotential. For this reason, this process can be considered as a potential method to fabricate single-crystalline nanowires of some materials that are difficult to be obtained in the conventional template-mediated electrodeposition.

Experimental Section

The Al film of high purity was deposited on the n-type silicon substrate (Silicon Inc., (100), $1-10 \Omega \text{ cm}$) by e-beam evaporation under the pressure of 10^{-6} Torr. A two-step anodization was conducted to improve the ordering of the channels in the PAA template.¹¹ To improve the filling efficiency, the barrier layer at the PAA/substrate interface was removed by immersing the anodized specimen into a 5 wt % H_3PO_4 solution at 30°C . In our previous study, the pore bases became arched at the alumina/Si interface when the Al film was consumed completely.¹² The formation of the arched pore base is beneficial

to the removal of the barrier layer because the barrier layer is partially destroyed. The barrier layer can thus be completely removed after chemical etching at 30°C for 20 minutes. A potentiostat (EG&G, model 263A) was also used to confirm the complete removal of the barrier layer by monitoring the current transient. The current density for the barrier layer-removed alumina/Si substrate is about 10 times that of the as-anodized one when the applied voltage is -3 V. The cathodic dc electrodeposition of Ni was performed in an aqueous solution composed of NiSO_4 (330 g/L), NiCl_2 (45 g/L) and H_3BO_3 (35 g/L). The working electrode, counter electrode and reference were the PAA/Si substrate, a platinum sheet and silver/silver chloride, respectively. The solution was not stirred during the whole electrodeposition process. After electrodeposition, a Ni layer containing nanostructures could be obtained by removing the PAA template in a 5 wt % NaOH solution. For the sake of comparison, the electrochemical deposition of Ni was conducted on PAA with a conductive Au interlayer inserted between the PAA and the Si substrate. Some blank Si substrates were also used for electrodeposition to further understand the electrodeposition behaviors of Ni on the PAA/Si substrates. The morphologies of the electrodeposited specimens were observed by a scanning electron microscope (Hitachi S4100) and field emission transmission electron microscope (Hitachi FE-2000).

Results and Discussion

Figure 1 shows the current variations recorded for the electrodeposition of Ni for different substrate arrangement. For

the electrodeposition on the PAA/Si substrate with a conductive Au interlayer under the PAA template, the current variation revealed the typical three stages of the growth of nanowires,¹³ as shown in Figure 1a. Stage I indicates the deposition of Ni into the channels. Stage II shows the formation of caps at the end of nanowires outside the channel and stage III shows the formation of planar Ni layer on the PAA surface. Figure 1b shows the current variation for the electrodeposition of Ni on the 300 nm thick PAA/Si substrate without a conductive interlayer. The current decreased in the beginning and reached a steady state in the subsequent electrodeposition process for all the applied voltages, quite different from that shown in Figure 1a. This indicates that the deposition mechanisms of Ni were probably different for the different substrates. Besides, no obvious fluctuation in current was observed for the electrodeposition on the PAA/Si substrate without a conductive layer, even when the applied voltage was as negative as -40 V. Only a few bubbles were found on the electrode for all the electrodeposition voltages, implying that the hydrolysis of water on the PAA/Si substrate was quite low. It is not clear why the hydrolysis reaction cannot readily occur on the PAA/Si substrate without a conductive layer; however, the low degree of the hydrolysis reaction reduces the possibility of obstructing the electrodeposition at more negative voltages by gas bubbles.

To further investigate the electrodeposition behavior of Ni on the PAA/Si substrate without a conductive interlayer, the electrodeposition was also conducted on the blank Si substrate. Figure 2a shows the surface morphologies of a Si substrate after the electrodeposition of Ni at -2 V for 10 min. Some Ni particles were formed, but with a very low density of about 1.45×10^4 cm⁻². Even for a more negative applied voltage (-3 V), the density of Ni particles only slight increases (3.15×10^4 cm⁻²), accompanying the formation of Ni particles of larger size (Figure 2b). The dominant carriers of n-type Si are electrons. When a negative voltage was applied on the n-type Si (forward bias),¹⁴ the electrons should easily be driven to the Si/solution interface and reduce the metal ions to form the deposit. Nevertheless, the results of Figure 2a,b indicate that the deposit does not prefer to nucleate on the Si substrate. The low nucleation density of metal on the semiconductor can be attributed to the low interaction energy between the absorbed metal atom and the substrate, as well as the required larger critical nucleus size compared with that on the metallic substrate.¹⁵

Part c and d of Figure 2 show the surface morphologies of 300 nm thick PAA/Si substrates after electrodeposition. The densities of Ni particles were about 2.5×10^6 and 4×10^6 cm⁻² when the electrodeposition was conducted at -2 and -3 V, respectively. When a 600 nm thick PAA/Si substrate was used for electrodeposition, the densities of Ni particles were 7.7×10^5 and 1.18×10^6 cm⁻² for voltage at -2 and -3 V, respectively (Figure 2e,f). These results indicate that the density of Ni particles decreased with the increase of the PAA thickness. In our previous study, it was found that no deposit was observed on the pore wall and the underlying Si when the electrodeposition voltage was more positive than -2 V.¹¹ As the applied voltage was more negative than -2 V, Ni began to deposit at the outer surface of PAA instead of the underlying Si. It was suggested that the unusual electrodeposition behavior was caused by the electrical breakdown of PAA that would lead to the formation of negatively charged pore wall. It is well-known that the pore wall is composed of the pure oxide at the inner part and the anion-contaminated oxide at the outer part. The conductivity of the anion-contaminated oxide is higher than the

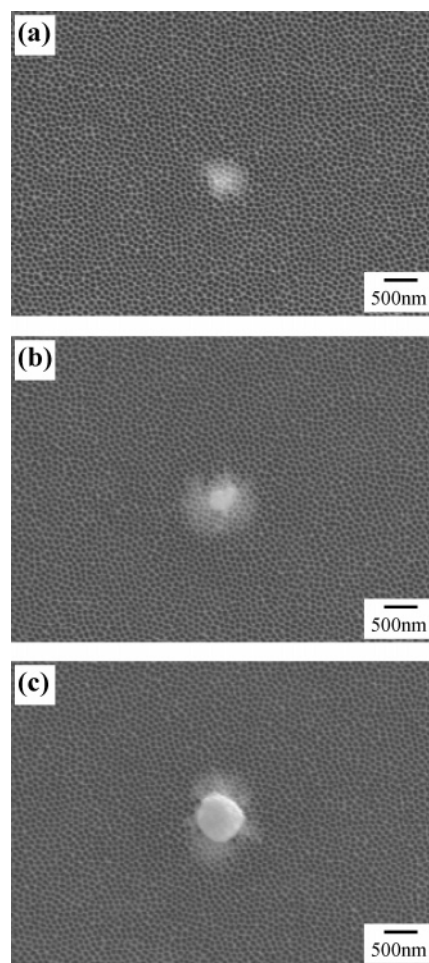


Figure 3. High-magnification image of 300 nm thick PAA surface in the initial period of electrodeposition at -2.0 V for (a) 30 s, (b) 90 s, and (c) 150 s.

pure oxide.¹⁶ Owing to the limited thickness of the template, electron avalanches due to the electrical breakdown of the anion-contaminated oxide might occur under the applied electrodeposition voltage in the present study, even though the calculated field strength was only about 10^5 V cm⁻¹ for the electrodeposition voltage of -3 V. The surface of the template could be considered as the cathode for electrodeposition. The electric field across PAA would decrease as the thickness of PAA was increased, leading to a reduced nucleation density of Ni because the nucleation density is dependent on the magnitude of overpotential.¹⁷

Another interesting phenomenon is that the density of Ni particles is higher on the PAA/Si substrate than that on the blank Si substrate under the same electrodeposition conditions. In addition to the factor of interaction energy mentioned above, other factors may also affect the electrodeposition of metal on the different substrates used. Because the pore wall of PAA is composed of pure oxide at the inner part and anion-contaminated oxide at the outer part,¹⁶ the existence of defects on the anion-contaminated oxide will provide more nucleation sites during electrodeposition. It may be one possible reason the density of Ni particle is higher on the PAA/Si substrate than that on the blank Si substrate.

Figure 3 shows a high-magnification image of a 300 nm thick PAA surface in the initial period of electrodeposition at -2.0 V. In the beginning, the deposition occurred in local area (the white area) on the PAA surface, like those shown in Figure 3a. The subsequent electrodeposition of Ni prefers to occur at the

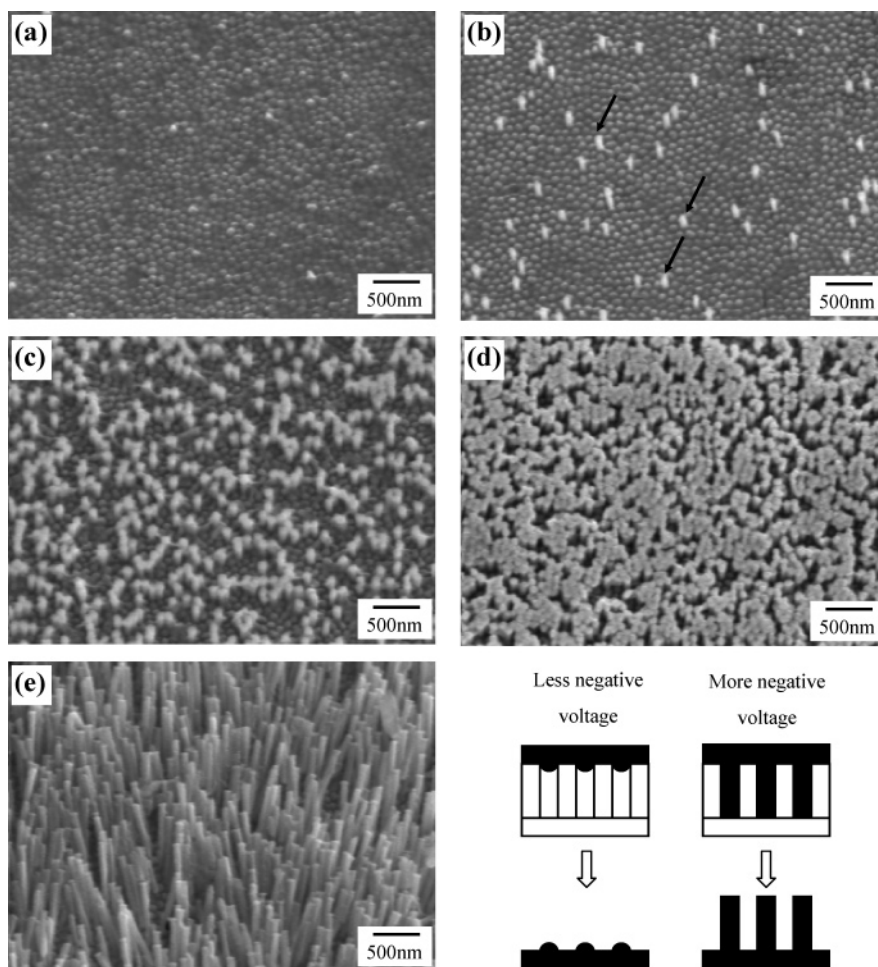


Figure 4. SEM images of the Ni layer containing nanostructures obtained at different voltages: (a) -2.0 V, (b) -8.0 V, (c) -20 V, (d) -40 V and (e) -40 V. The thickness of PAA used for images of (a)–(d) is 300 nm, and the thickness of PAA used for (e) is 600 nm.

deposited regions, leading to the growth of Ni particles, as shown in Figure 3b,c. Two important issues were revealed from the results in Figures 2 and 3. First, the electrical breakdown occurs randomly at local regions of PAA. The density of the breakdown regions increases with the applied voltage. Nucleation will first occur at these breakdown sites, unlike the homogeneous nucleation of deposit on a conductive substrate. Second, in the prolonged electrodeposition, a continuous planar Ni layer will be observed on the PAA surface, implying that the formation of the Ni layer is contributed by the continuous nucleation and lateral growth of the as-grown Ni particles.

After the electrodeposition, the PAA template was removed by immersing the specimen in a 0.5 wt % NaOH solution and the Ni layer containing nanostructures was observed from the side facing the PAA/Si interface, as shown in the schematic diagram of Figure 4. Figure 4a–d shows the Ni nanostructures obtained under various voltages on the 300 nm thick PAA/Si substrates. At a less negative voltage (-2.0 V), only Ni nanodots could be observed on the backside of the Ni deposit, implying that the filling of ions into pores was terminated soon after the beginning of the electrodeposition. When the applied voltage became more negative (-8 V), some Ni nanowires were formed in addition to nanodots, like those indicated by arrows in Figure 4b. The fraction of nanowires in the deposits increased when the applied voltage became more negative, as shown in Figure 4c,d. Similar deposition behaviors were also observed if a 600 nm thick PAA/Si substrate replaced the 300 nm thick one. Figure 4e shows the Ni nanowires obtained on the 600 nm thick PAA/Si substrate (the electrodeposition voltage was -40 V). The

diameter and the length of the nanowires are 60 and 600 nm, respectively, coinciding with the characteristics of the PAA template. These results indicate that most of the channels of PAA can be completely filled as the electrodeposition voltage is negative enough, though there is no conductive layer introduced between PAA and Si substrate.

As mentioned above, the electrodeposition of Ni on the PAA substrate without a conductive interlayer is contributed by the electrical breakdown of the PAA template. The electron avalanches caused by the electrical breakdown transformed the PAA substrates to be negatively charged, which in turn could be the cathode for the electrodeposition of Ni. Owing to the geometry factor, the electric field at the pore mouth would be higher than that at the pore walls, implying that the deposition rate of Ni would be higher at the pore mouth. Moreover, at a less negative voltage, the migration of ions into channels driven by the electric field is low. Therefore, the deposition of Ni into channels would be self-terminated at the electrical breakdown regions and keep on growing laterally till the metal spread over the whole electrode area, leading to the formation of Ni nanodots by the partial filling of the pores near the top surfaces.

At a more negative voltage (-8 V), the pore walls of some channels would suffer severe electron avalanches and be highly negatively charged, enhancing the migration of ions into these channels. Some channels were completely filled during electrodeposition and formed nanowires, like those shown in Figure 4b. As the voltage became much more negative (20 – 40 V), the fraction of pores with highly negatively charged pore wall would increase and more pores could be completely filled during

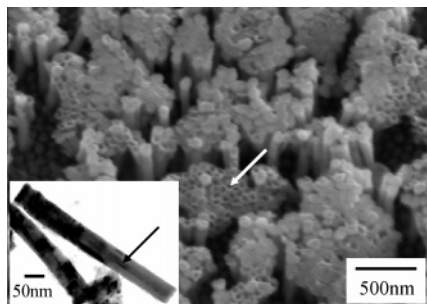


Figure 5. Morphologies of Ni nanowires and nanotubes obtained at -40 V on the 600 nm thick PAA/Si substrate.

electrodeposition. In fact, the density of Ni nanowires also increased with the increase of the applied voltage, as shown in Figure 4c,d.

Except the nanowires, some nanotubes were also formed as the electrodeposition was conducted at -40 V, as shown in Figure 5. The inset in Figure 5 shows the TEM image of the nanotube, indicating that the one-dimensional structure is hollow. Because the electrodeposition was contributed by the electrical breakdown of the template, the pore walls were highly negatively charged at a more negative voltage. The electrodeposition could first occur on the whole surface of the pore walls, followed by the growth of Ni toward the center of the channel. Some pore mouths may be closed before the channels were completely filled, leading to the formation of the nanotubes. As the pore mouths were closed after the channels were completely filled, the nanowires were formed. Figure 5 can further confirm that the deposition began on the pore wall instead of from the bottom of the channel if the electrodeposition was conducted at a more negative voltage. The results in Figures 4 and 5 revealed that the electrodeposition behaviors on the PAA/Si substrate without a conductive interlayer are mainly voltage-dependent, but not time-dependent.

Finally, another unusual phenomenon different from those obtained in the conventional template-mediated deposition

deserves to be mentioned here. Figure 6 shows the TEM images of Ni nanowires formed at -40 V. Parts a and b of Figure 6 show the low-magnification image and high-resolution lattice image of polycrystalline Ni nanowires, respectively. It is clear that a single nanowire was composed of many grains. Several rings can be observed in the electron diffraction pattern (the inset of Figure 6b), indicating that the nanowire is polycrystalline. Except for the polycrystalline ones, some single-crystalline Ni nanowires were also formed at -40 V. Parts c and d of Figure 6 show the low-magnification image and high-resolution lattice image of single-crystalline Ni nanowires, respectively. The diffraction patterns obtained at the different points of a single nanowire are all the same, implying that the nanowire is single-crystalline. For the preparation of metal nanowires, the growth of single-crystalline nanowires is related to the 2D nucleation.¹⁸ During electrodeposition, generally, new grains will grow when the size of nucleus exceeds the critical dimension N_c .¹⁹ A larger N_c is favorable to the growth of a single crystal. For the 2D-nucleation, the critical dimension N_c can be expressed as $N_c = bse^2/(Z\eta)^2$, where b , s , ϵ , Z , and η are a constant, the area occupied by one atom on the surface of the nucleus, the edge energy, the effective electron number and the overpotential,¹⁹ respectively. During electrodeposition, the only parameter one can control directly is the overpotential η . A low η is favorable for the growth of the single-crystal because N_c is large. However, in our study, single-crystalline nanowires could also be formed even under a very large overpotential. Therefore, there must be some other factors that affect the formation of the single-crystalline nanowires on the PAA/Si substrate. Except for the nucleation conditions, the growth of the nanowire is also time-dependent. A very large overpotential (for example, -40 V in the present study) may prefer the growth of new grains during electrodeposition. However, for the electrodeposition on the PAA/Si without a conductive layer, Ni ions would be strongly driven into some channels with highly negatively charged pore walls. These pores were completely filled rapidly before the growth of a second grain, leading to the formation

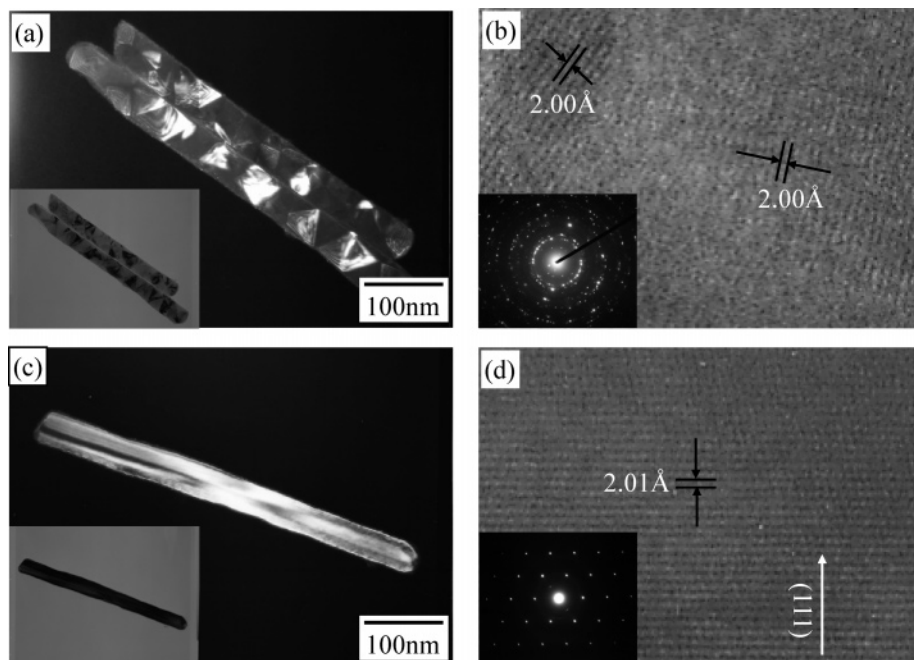


Figure 6. TEM images of Ni nanowires obtained under the electrodeposition at -40 V: (a) bright field and dark field images of the polycrystalline Ni nanowire, (b) high-resolution lattice image of the polycrystalline Ni nanowire, (c) bright field and dark field images of the single-crystalline Ni nanowire, and (d) high-resolution lattice image of the single-crystalline Ni nanowire. The insets in images (b) and (d) show the diffraction patterns of polycrystalline and single-crystalline Ni nanowires, respectively.

of the single-crystalline nanowires. Therefore, it is believed that this process is beneficial to the preparation of single-crystalline nanowires that are difficult to obtain by conventional template-mediated techniques.

Conclusion

In the present study, an unusual electrodeposition behavior on the PAA/Si without a conductive layer between the template and Si was described. The current decreased continuously during the whole electrodeposition process, unlike that obtained on the PAA/Si substrate with a conductive layer between the template and Si. No obvious hydrolysis of water on the substrate surface was observed even when the applied voltage was as negative as -40 V. The deposition occurred at the local regions of PAA in the beginning, and a planar Ni layer was finally formed due to the continuous nucleation and lateral growth of Ni particles. At a less negative voltage (-2 V), a Ni layer containing only nanodots was formed. As the electrodeposition voltage became more negative, some nanowires would also be formed and the density of nanowires increased with the increase of the applied voltages. Besides the polycrystalline nanowires, some single-crystalline nanowires were also formed when the electrodeposition voltage was -40 V. The results in the present study show that the electrodeposition behaviors on the PAA/Si substrate without a conductive layer between the template and Si are mainly voltage-dependent.

Acknowledgment. We acknowledge the financial support from the National Science Council of the Taiwan, Republic of China under Contract No. NSC 92-2120-M-006-003.

References and Notes

(1) Cao, H.; Qiu, X.; Luo, B.; Liang, Y.; Zhang, Y.; Tan, R.; Zhao, M.; Zhu Q. *Adv. Funct. Mater.* **2004**, *14*, 243–246.

- (2) Keating, C. D.; Natan, M. J. *Adv. Mater.* **2003**, *15*, 451–454.
- (3) Dick, B.; Sit, J. C.; Brett, M. J.; Votte, I. M. N.; Bastiaansen, C. W. M. *Nano Lett.* **2001**, *1*, 71–73.
- (4) Jessensky, O.; Müller, F.; Gösele, U. *J. Electrochem. Soc.* **1998**, *145*, 3735–3740.
- (5) Li, A. P.; Müller, F.; Birner, A.; Nielsch, K.; Gösele, U. *J. Appl. Phys.* **1998**, *84*, 6023–6026.
- (6) Hobbs, K. L.; Larson, P. R.; Lian, G. D.; Keay, J. C.; Johnson, M. B. *Nano Lett.* **2004**, *4*, 167–171.
- (7) Lakshmi, B. B.; Dorhout, P. K.; Martin, C. R. *Chem. Mater.* **1997**, *9*, 857–862.
- (8) Wang, Y. C.; Leu, I. C.; Hon, M. H. *J. Mater. Chem.*, **2002**, *12*, 2439–2444.
- (9) Yi, G.; Schwarzacher, W. *Appl. Phys. Lett.* **1999**, *74*, 1746–1748.
- (10) Zhang, J.; Wang, X.; Peng, X.; Zhang, L. *Appl. Phys. A* **2002**, *75*, 485–488.
- (11) Wu, M. T.; Leu, I. C.; Yen, J. H.; Hon, M. H. *Electrochem. Solid State Lett.* **2004**, *7*, C61–C63.
- (12) Wu, M. T.; Leu, I. C.; Hon, M. H. *J. Mater. Res.* **2004**, *19*, 888–895.
- (13) Ohgai, T.; Hoffer, X.; Fabian, A.; Gravier, L.; Ansermet, J.-P. *J. Mater. Chem.* **2003**, *13*, 2530–2534.
- (14) Plummer, J. D.; Deal, M. D.; Griffin, P. B. *Silicon VLSI Technology*; Prentice Hall Inc.: Upper Saddle River, NJ, 2000; Chapter 1.
- (15) Oskam, G.; Long, J. G.; Natarajan, A.; Searson, P. C. *J. Phys. D: Appl. Phys.* **1998**, *31*, 1927–1949.
- (16) Thompson, G. E.; Wood, G. C. *Treatise on Materials Science and Technology, Corrosion: Aqueous Processes and Passive Films*; Academic Press Inc. Ltd.: London, 1983; Vol. 23, Chapter 5.
- (17) Budevski, E.; Staikov, G.; Lorenz, W. J. *Electrochemical Phase Formation and Growth*; Weinheim-VCH: Weinheim, 1996; Chapter 3.
- (18) Tian, M.; Wang, J.; Kurtz, J.; Mallouk, T. E.; Chan, M. H. W. *Nano Lett.* **2003**, *3*, 919–923.
- (19) Paunovic, M.; Schlesinger, M. *Fundamental of Electrochemical Deposition*; Wiley: New York, 1998; p 108.